SCI. MAR., 65 (Suppl. 1): 291-300 SCIENTIA MARINA 2001

AN INTERDISCIPLINARY VIEW OF THE OCEAN. *J.L. PELEGRÍ, I. ALONSO and J. ARÍSTEGUI (eds.)*

Vertical velocities at an ocean front*

PEDRO VÉLEZ-BELCHÍ[1,2] and JOAQUÍN TINTORÉ[2]

[1]Instituto Español de Oceanografía, Tenerife, España.
[2]Instituto Mediterráneo de Estudios Avanzados (CSIC-UIB), Palma de Mallorca, España.

SUMMARY: Simple scaling arguments conclude that the dominant motions in the ocean are horizontal. However, the vertical velocity plays a crucial role, connecting the active upper layer with the deep ocean. Vertical velocities are mostly associated with the existence of non-transient atmospheric wind forcing or with the presence of mesoscale features. The former are the well known upwelling areas, usually found at the eastern side of the oceans and characterised by upward vertical velocities. The latter have been observed more recently in a number of areas of the world's oceans, where the vertical velocity has been found to be of the order of several tens of meters per day, that is, an order of magnitude higher than the largest vertical velocity usually observed in upwelling areas. Nevertheless, at present, vertical velocities cannot be measured and indirect methods are therefore needed to estimate them. In this paper, the vertical velocity field is inferred via the quasi-geostrophic omega equation, using density data from a quasi-permanent upper ocean front located at the northern part of the western Alborán gyre.

Key words: vertical velocities, mesoscale circulation, upper ocean front, western Alborán gyre.

INTRODUCTION

Importance of vertical motions in the ocean

It is well known that, except in some small areas, the open ocean can be considered as a biological desert (Williams and Follows, 1998). In fact, about 90% of the world's fisheries are obtained in less than 2% of the total area of the world's ocean, the upwelling regions. This can be easily understood because oceanic motions are mainly horizontal, with little connection between the upper and the deep ocean. These layers can be considered complementary, in a biological sense, since in the upper one the presence of light permits life, while the deep layers are usually rich in nutrients. Consequently, the relevance of the vertical velocities (w) comes from the fact that they connect the nutrient rich deep ocean to the upper layer, where light makes life possible.

*Received October 29, 1999. Accepted September 20, 2000.

Different types of vertical motions

Vertical velocities important for the biological activity can be forced either by wind or by mesoscale activity. In case of wind-induced w, the combined effect of the equatorwards winds and the Coriolis force drives coastal surface waters offshore, and subsurface waters ascend as a compensation into the surface layer. The upwelled waters do not come from great depth, usually from no deeper than 200-300 m. When the upwelled waters are rich in nutrients, biological activity may be promoted. Examples of regions where wind-induced upwelling takes place are the eastern boundary of the oceans:

the west coast of north and central America (California and Peru), the coast of west Africa and the Atlantic side of the Iberian Peninsula (Barton *et al.*, 1998; Flament *et al.*, 1985; Huyer, 1976; Mittelstaedt, 1983).

Mesoscale-induced vertical velocities

There is another type of vertical velocities which are important for biological activity: those associated with mesoscale features, mainly eddies and instabilities of ocean currents.

In the ocean, there is a natural horizontal scale determined by the dynamical balance between the Coriolis and pressure forces. This horizontal scale is known as the Rossby internal deformation radius (Gill, 1982). Mesoscale processes can be roughly defined as those with spatial scales of the order of the Rossby radius. The mesoscale is known as the 'oceanic weather', and develops more energy than any other motion in the ocean (Robinson, 1983). The high spatial and temporal variability associated with mesoscale motions gives rise to the existence of areas of convergence and divergence, and consequently to the existence of intense upwelling and downwelling areas. The existence of vertical velocities in mesoscale oceanic features has been established in recent years in a number of areas of the world's oceans (Deway *et al.*, 1991; Tintoré *et al.*, 1991; Pinot *et al.*, 1995). The vertical velocities found are of the order of several tens of metres per day, that is, an order of magnitude higher than the largest vertical velocities usually observed in upwelling areas. Clear biological implications such as the enhancement of primary production have been found (Strass, 1992; Ruíz *et al.*, 1996; Blanco *et al.*, 1994; Vélez-Belchí *et al.*, 1998). The role of *w* is not only in a biological sense, it is also crucial for understanding frontogenesis processes, as different numerical studies have suggested (Onken, 1992; Wang, 1993; Strass 1994; Wang and Ikeda, 1997). However, vertical velocities cannot be measured directly (at least in an Eulerian framework). In the last fewyears, theoretical advances have permitted the estimation of *w* from density data (Holton, 1992; Hoskins *et al.*, 1978; Hoskins *et al.*, 1985). Usually, the vertical velocity is inferred using the omega equation that assumes quasi-geostrophic dynamics. This formulation has been used by several authors in different regions of the world's oceans (Dewey *et al.*, 1991; Pinot *et al.*, 1995; Viúdez *et al.*, 1996a, b). Leach (1987) applied a two-dimensional version of the omega equation to estimate vertical motions, and Tintoré *et al.* (1991) showed that the magnitude of vertical motions depends on the horizontal scale of the instabilities. The reliability of the omega equation as a method for estimating vertical velocities from density data was analysed by Pinot *et al.* (1996) and Strass (1994). Consistent estimates were also made from RAFOS floats, current meters and IES by Lindstrom and Watts (1994). In these studies, the *w* estimations were made with a dataset not collected for that purpose, hence in 1996 an experiment (called Omega) was carried out to specifically test the validity of the vertical velocity fields estimated using indirect methods. Therefore, the objective of this paper is to diagnose and describe the vertical velocities associated with mesoscale features, using the omega equation in a dataset specially designed to establish the validity of the quasi-geostrophic method for estimating *w*. Given the multidisciplinary nature of the field study and of this special issue, we will also describe the mechanism that produces vertical velocities at the mesoscale, emphasising the differences from the vertical motions suggested by the isopycnals.

The remainder of this paper is organised as follows. First we describe the dataset and the sampling methods, and present the thermohaline structure as inferred from the hydrographic data. Next, the basic theory and underlying physics, that explain the existence of vertical velocities in mesoscale features, are outlined. Afterwards, we present the diagnosis of the vertical velocity and examine the full three-dimensional pathway of water parcels passing through the region. Finally, the results are discussed and the conclusions presented.

DATA SET

The Omega field experiment was carried out from the 1 to 15 October 1996 on board the Spanish R/V Hespérides in the western Alborán sea. Data from satellite sea surface temperature were used to locate the northern part of the western Alborán gyre (hereafter, WAG). To resolve both the spatial and temporal variability of the upper 300 m, four small scale surveys were carried out in the same area. This paper discusses the results of the analysis applied to data obtained in the first survey, leaving the analysis of the additional dataset to future studies. The first small-scale survey was conducted on 2-4 October

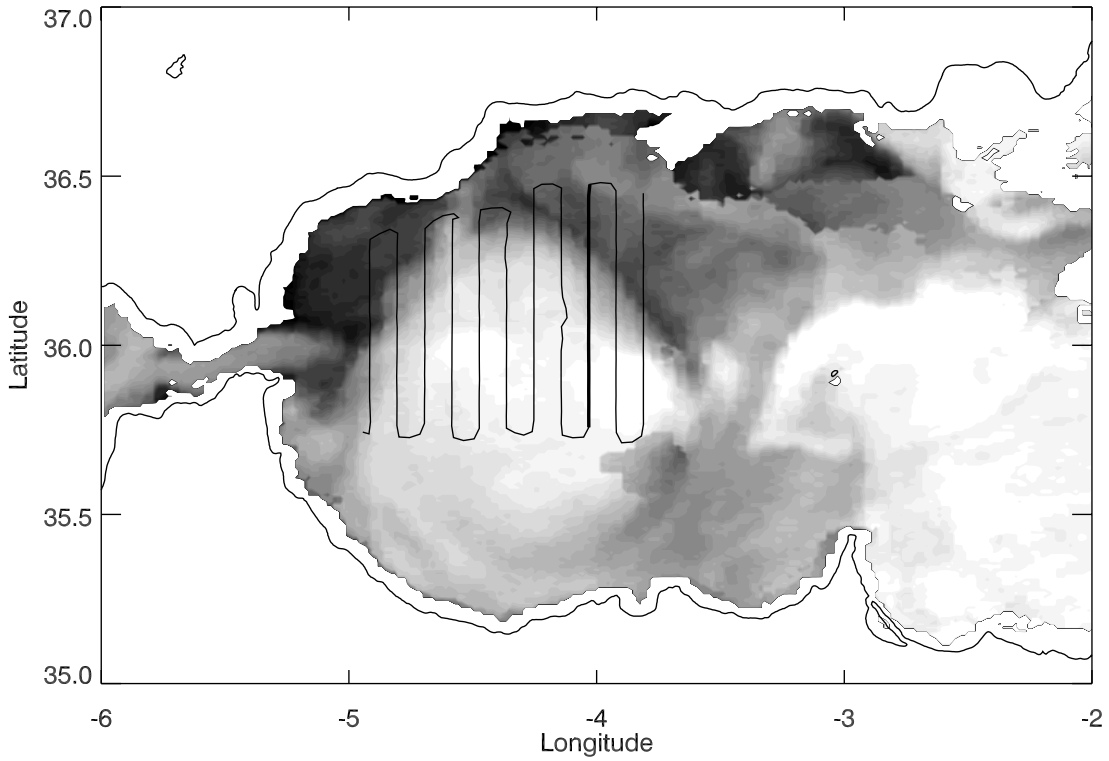

FIG. 1. – Satellite sea surface temperature of the Alborán Sea (2 October 1996). Light colours mean warmer waters. The ship track for the first survey is overlaid. The location of the 4.03ºW meridional section is indicated by a thick line.

and was composed of ten meridional sections 70/80 km long and separated by 10 km in the west-east direction. Figure 1 shows the sea surface temperature image for 2 October 1996 with the cruise track. The survey covered a rectangular area of about 80 km by 100 km, centred at around 4.4ºW 36ºN, and took 68 hours to complete. The physical field was sampled using a SeaSoar that carried out a conductivity-temperature-depth (CTD) sensor, a fluorometer and a light sensor. The SeaSoar undulated between the surface and the 350 m level, an undulation being completed every 4 km. The raw SeaSoar data were averaged into 8 dbar bins with an along-track resolution of 4 km. Absolute currents were measured using a vessel mounted 150 kHz RDI ADCP. The raw ADCP data were merged with differential GPS positions and averaged in time to obtain accurate absolute velocities with an along-track resolution of 2 km and binned in 8 m cells. A complete description of SeaSoar CTD and ADCP data processing is contained in the data report by Allen *et al*. (1997).

During the first survey, neutrally buoyant Lagrangian floats were deployed at the depth where maximum vertical motion was expected (100 m), providing direct Lagrangian estimates of the vertical velocity.

THERMOHALINE STRUCTURE

In this section, the high resolution CTD profiles obtained from the SeaSoar hydrographic survey will be used to briefly describe the thermohaline structure of the northern part of the WAG. This description is useful to understand the dynamical conditions needed for the establishment of a significant vertical velocity field, but a detailed description of the hydrographic features in the Omega experiment is beyond the scope of the present paper.

In the Alborán sea two very different water masses are present (Cano and Castillejo, 1972; Lanoix, 1974), the dense Mediterranean waters (MW, S>38.2) and the light modified Atlantic waters (MAW, S<36.5), which are the result of the mixing between the north Atlantic central waters (NACW, S<36.45) and the MAW (Gascard and Richez, 1985). The horizontal distribution of density (Fig. 2) shows the existence of a front that separates the dense waters in the north from a bowl of light waters placed in the south. This bowl of light waters, mainly MAW, constitutes an anticyclonic vortex, known as the western Alborán Gyre. As can be observed in Figure 2, the density front extends down to 200 dbar. At 50 dbar (Fig. 2a), the bowl of MAW is homogenous, with densities smaller than 26.0 kg m^{-3}. At 100

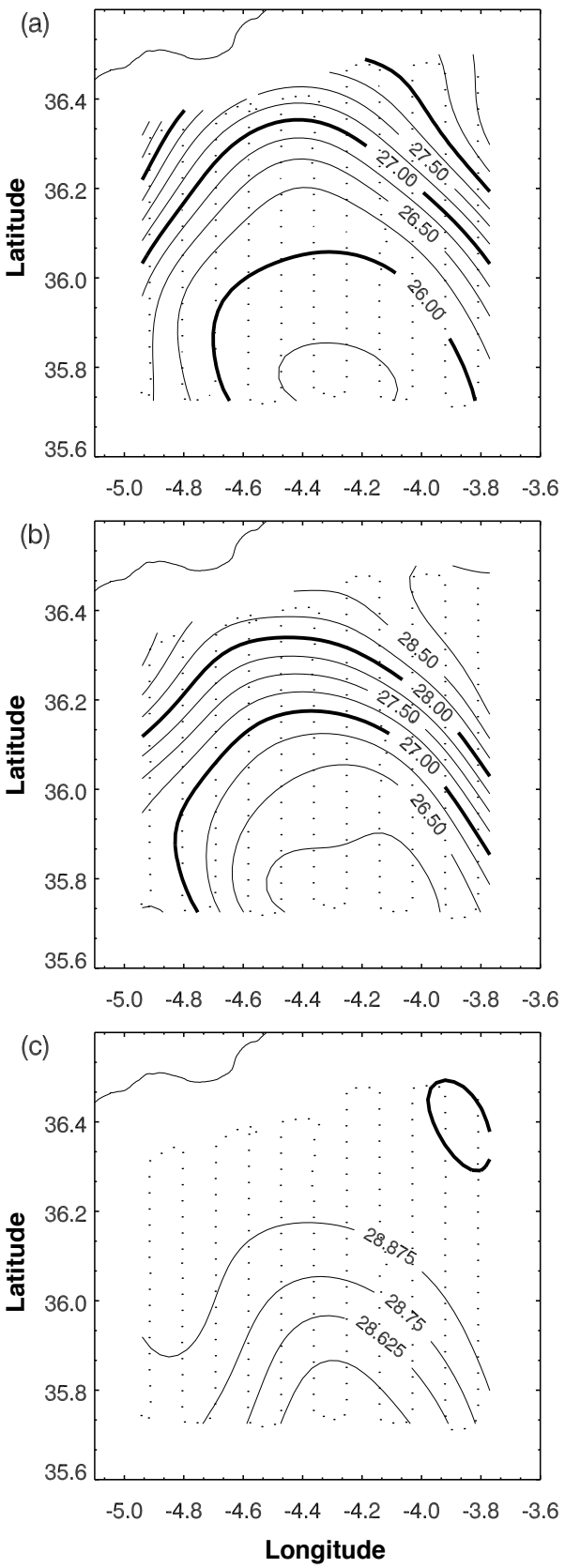

FIG. 2. – Maps of objectively analysed sigma$_t$ (kg m^{-3}) at (a) 50 dbar, (b) 100 dbar and (c) 200 dbar. The location of the SeaSoar measurements are shown as small dots.

dbar (see Fig. 2b), the horizontal gradient of the front is 1.8 kg m^{-3} in 20 km, that is, about 2 kg m^{-3} in one Rossby radius, a gradient comparable to the strongest gradients found in the world's oceans. At 200 dbar, the WAG is still present, although the density gradients are weak. At this level the sampled region is mainly occupied by dense MW.

A south-north section of density (see Fig. 3) shows that the core of light waters (the WAG) extends from the surface down to 200 dbar, and is separated from the Mediterranean waters by a strong pycnocline that ranges from roughly 50 dbar at 36.4ºN to about 160 dbar at the southern part, 35.8ºN. The vertical gradients of the pycnocline are up to 1 kg/m^3 in 40 dbar (between the 27.0 kg m^{-3} and the 28.0 kg m^{-3} isopycnals) at the base of the WAG, near 35.8ºN. Associated with the density front is an intense jet: the Atlantic jet (hereafter AJ). Figure 3b shows a south-north section of eastward ADCP velocity, maximum ADCP velocities being found in the top 50 dbar, reaching magnitudes of up to 110 cm/s. The AJ extends down to 200 dbar, the level at which the density front has almost disappeared. In addition to the AJ-WAG system, there are several interesting small-scale features, such as the small anticyclonic eddy at the south-west corner (4.9ºW 35.7ºN) and the cyclonic circulation in the north-east corner (3.8ºW 36.4ºN).

In summary, the western Alborán sea is dominated by the presence of an eastward jet that surrounds a large anticyclonic gyre. Therefore, the Alborán sea is a case area in which the existence of a quasi-permanent front due to interaction between different water masses makes it ideal for estimating vertical velocities.

VERTICAL VELOCITIES

In this section, we will describe the basic mechanism that explains the distribution of vertical velocities in mesoscale structures, emphasising the relationship between the *w* distribution and the density field.

The first order approximation to understand the ocean's behaviour is the well-known geostrophic balance. As this solution is the final steady-state towards which the ocean tends to adjust, it is not suitable for explaining time-dependent features such as the mesoscale ones. The way the ocean adjusts to slow changes (time scale >> f^{-1}) is of vital importance for an understand of mesoscale evolution. The key to understanding slow adjustment is to deter-

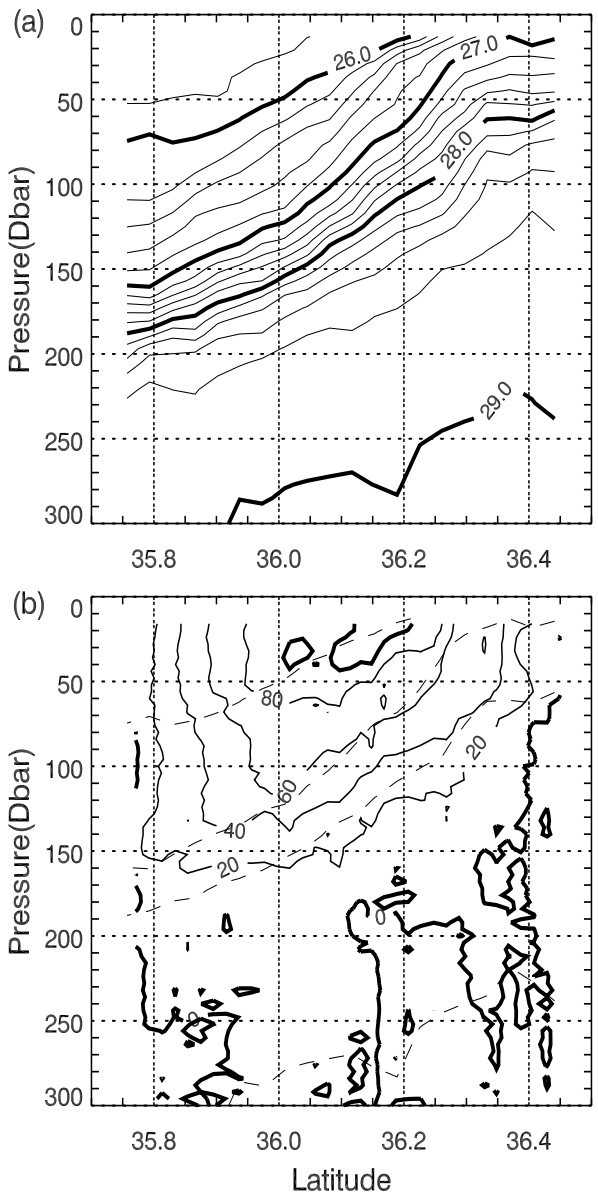

FIG. 3. – South-north section of (a) sigma$_t$ (kg m^{-3}) and (b) eastward ADCP velocity(cm/s) at 4.03ºW. In the second figure, the density is overlaid for reference.

mine the departures from geostrophy, even though they are small. Hence, a higher order approximation is needed, leading to what is known as the quasi-geostrophic theory. The time evolution in this theory is dominated by the geostrophic advection of momentum and density, and the twin requirements of geostrophic and hydrostatic balance constrain the balance. In other words, the slow evolution of mesoscale features is driven by the geostrophic advection of density and momentum, advection that modifies the initial fields, hence the geostrophic and hydrostatic balance could be violated. Since the ocean at scales larger than the Rossby radius is almost in geostrophic and hydrostatic balance, the density field must be modified through the vertical velocity field. Therefore, the *w* field is the requirement to ensure that the changes in the density field during the time evolution of mesoscale features will keep the thermal balance valid. In summary, from the point of view of the quasi-geostrophic theory, the slow evolution of a mesoscale feature can be described as a process that tends towards geostrophic and hydrostatic balance but is continuously altered.

This complex tendency to a balance can be written in a mathematical sense (Holton, 1992; Hoskins *et al*., 1978; Hoskins *et al*., 1985), yielding equations that describe the time evolution of the geopotential and the vertical velocity field. At each time, the vertical velocity will be given by the diagnostic omega equation:

$$N^2\nabla_h w + f_0^2\frac{\partial^2 w}{\partial z^2} = \\ = f_0\frac{\partial}{\partial z}\left(\vec{v}_g\cdot\nabla_h\xi_g\right) + \frac{g}{\rho}\nabla^2\left(\vec{v}_g\cdot\nabla_h\rho\right) \qquad (1)$$

where ρ is the density field, N is the Brunt-Väisälä frequency, g is the gravity, f_0 is the Coriolis parameter, $\vec{v}_g$ is the geostrophic velocity computed from the geopotential and ξ_g is the geostrophic vorticity.

The two terms on the right hand side of Equation 1 are associated with the two components of the vertical velocity: along-isopycnal advection and local isopycnal displacement. Local isopycnal displacement is related to the in-situ change of the isopycnal positions. For instance, the motion of a cyclonic eddy will produce a lifting of the isopycnal, but this does not mean that all the water on top will be displaced upwards, since the flow is basically geostrophic and therefore horizontal. This is consistent with the fact that a quasi-stationary cyclonic eddy does not mean permanent upward motions at its centre. On the other hand, along isopycnal advection is induced by the small horizontal departures from the geostrophic velocity (ageostrophic horizontal velocity), which push the water parcels out of their isopycnal. Then, in their aim to keep their density constant, water parcels undergo vertical excursions, either upward or downward. Figure 4 shows a sketch of the vertical velocity field in an ideal theoretical situation of a growing baroclinic meander. The meander is defined by the

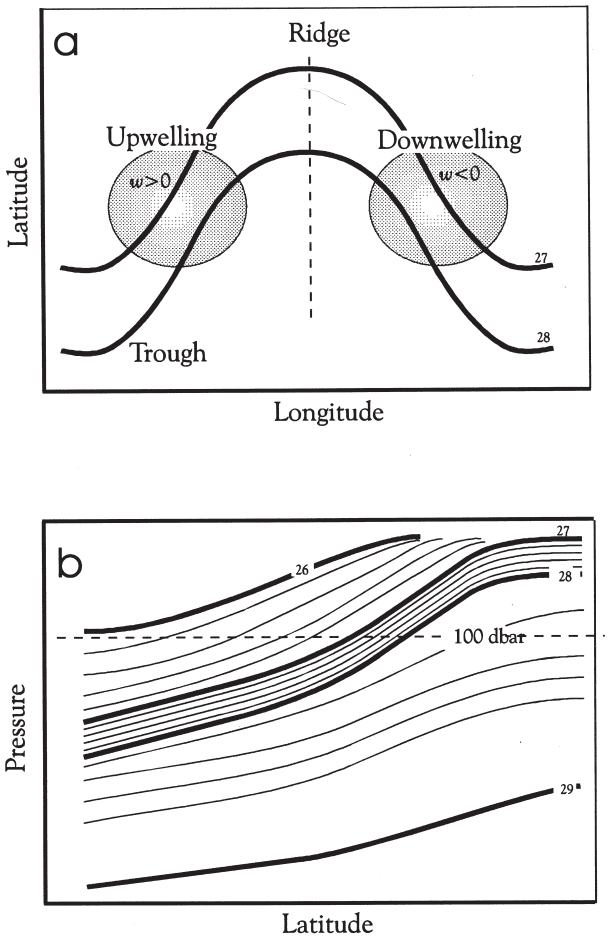

FIG. 4. – a) Schematic diagram of the vertical velocity field at 100 dbar during the developing phase of a baroclinic meander. The thick lines are the isopynals that define the menader Upwelling (downwelling) occurs to the west (east) of the wave ridge. b) Schematic South-North vertical section of density at the position indicated by the dashed line in (a).

27.0 kg m^{-3} and 28.0 kg m^{-3} isopycnals, while the position of the *w* maximum and minimum are denoted by a circle. Note that the present diagram is for the developing phase of the meander; during a mature or decaying phase of the baroclinic meander (or a detached eddy) the upwelling (downwelling) occurs in the ridge (trough).

A detailed description of the quasi-geostrophic theory is beyond the scope of the present section (for a detailed explanation see Holton, 1992), but two ideas should be stressed: *w* is needed to keep the ocean near hydrostatic and geostrophic balance; and the geostrophic velocity does not produce along-isopycnal advection (climbing up the isopycnal surface) and consequently the vertical velocity cannot be inferred from just vertical sections of density. These concepts will be illustrated with experimental data in the following section.

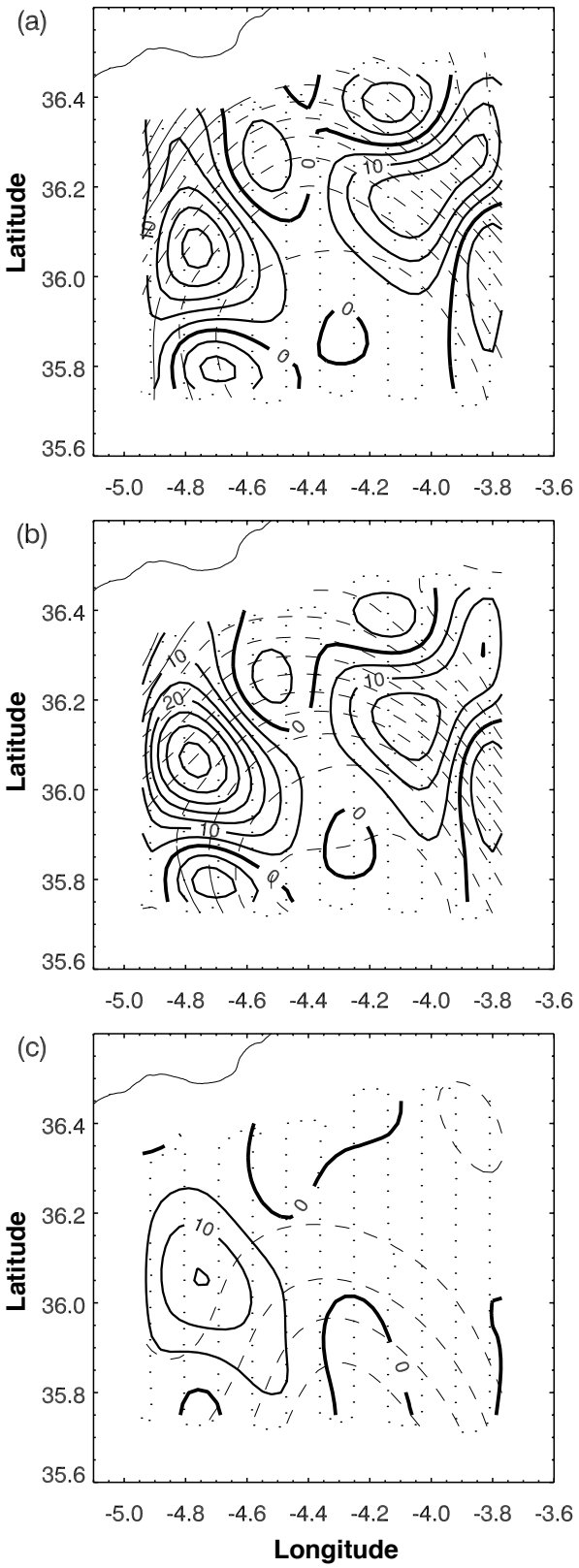

FIG. 5. – Maps of vertical velocity (m/day) calculated from the objectively analysed density data via the quasi-geostrophic omega equation at (a) 50 dbar, (b) 100 dbar and (c) 200 dbar. The 26, 27, 28 and 29 kg m^{-3} isopycnals are overlaid for reference as dashed lines.

RESULTS

To estimate vertical velocities using the omega equations, we need to compute high-order spatial derivatives of the density field (such as vorticity). Hence, the SeaSoar data should be gridded and smoothed to avoid amplifying small-scale noise, such as internal waves and inertial oscillations. The procedure for obtaining the smooth and gridded density field can be summarised as follows: first, a residual field is calculated by subtracting the mean field from the raw data; then, the residual field is interpolated onto a regular grid and smoothed using an objective analysis method called 'successive corrections' (Pedder, 1989, 1993). Finally, the total density field is computed adding the objectively analysed residual and the mean field.

From the density field, the geostrophic velocities can be computed via the thermal wind relation, assuming a level of no motion at 300 dbar, and then the omega equation can be solved using w=0 as boundary conditions. The diagnosed vertical velocity is shown in Figure 5. The density field is overlaid to show the relationship between the two variables. At 100 dbar the diagnosed w is characterised by a large upwelling patch that extends from west to east. There are also some 20 km sized patches of downwelling, placed in the north and in the south-west. This last patch is due to the change in curvature associated with the small eddy placed near 4.8°W 35.8°N. The strongest vertical velocities are located within the jet, the maximum values reaching 40 m/day in the areas where curvature and advection are maximum. The weak vertical velocities within the core of the WAG are consistent with the low-energy character of the inner part of a big anticyclonic eddy such as the WAG. The described horizontal distribution has the same features at deeper and shallower levels (Figs. 5a and 5c), although the magnitudes are weaker. At 200 dbar, the maximum values reach 15 m/day, while the minimum value is around -2 m/day.

The vertical distribution of w is represented along 4.03ºW in Figure 6, being characterised by an upwelling maximum of 20 m/day centred at 75 dbar and by a downwelling maximum of about –7m/day at 50 dbar. The vertical distribution is of one sign between the surface and 300 dbar. Fig. 6 shows that the downwelling/upwelling maximum does not occur at the place where the tilting of the isopycnals is minimum/maximum; moreover, light water is being upwelled while dense water is being downwelled, a process that tends to stratify the water column. In contrast with the ideal situation of Fig. 4, the diagnosed w field is not symmetric with respect to the ridge. The differences are basically due to

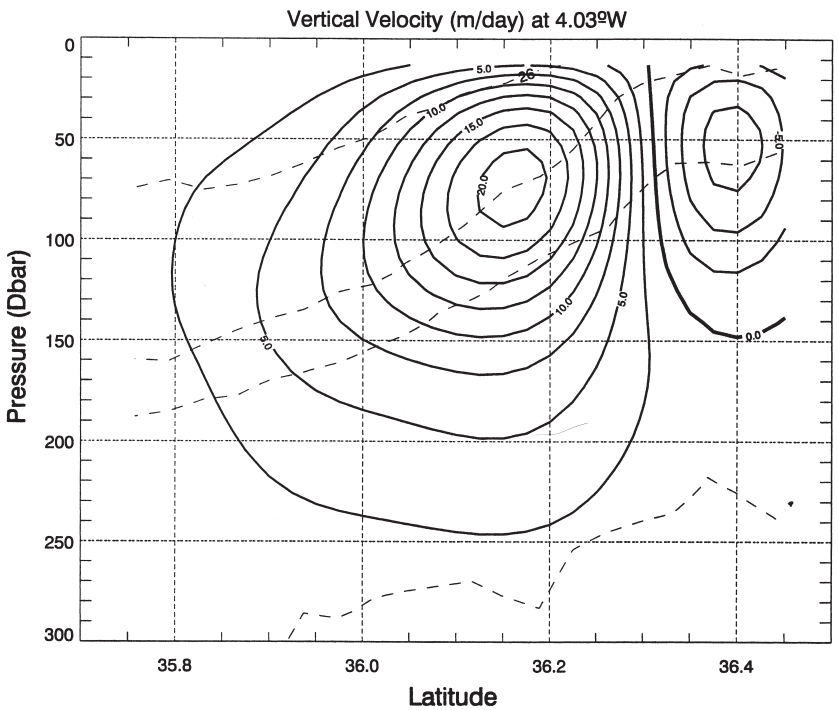

FIG. 6. – South-north section of vertical velocity (m/day) along the 4.03ºW meridian. The 26, 27, 28 and 29 kg m^{-3} isopycnals are overlaid for reference as dashed lines.

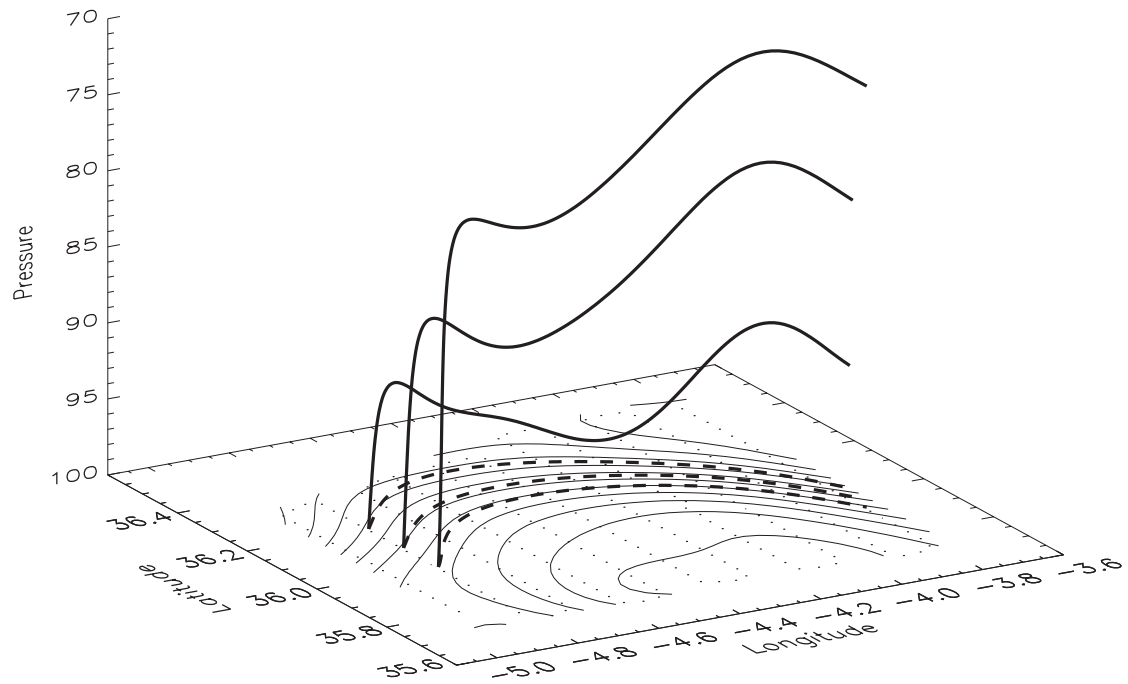

FIG. 7. – Three dimensional streamlines (heavy solid line). In the case of stationary fields, streamlines coincide with water particle trajectories. For reference we also include projections (heavy dashed line) of the streamlines plotted over the sigma$_t$ field at 100dbar.

both the state of the WAG (which is not growing but could be considered as an eddy in a quasi-stationary phase) and the effect of small changes in the curvature of the jet (the predominant factors that modify the structures of advection and therefore of *w)*.

Due to inertial currents and baroclinic tidal currents found in the western Alborán sea, the horizontal velocities obtained with the ADCP do not have enough accuracy to diagnose vertical velocities through the divergence equation. Therefore, the ADCP data set cannot be used to validate the vertical velocity field.

The diagnosis of vertical velocities has shown strong velocities associated with the Atlantic jet. However, in terms of enhancing the biological activity, what is important is how a water parcel would move trough the region. As water parcels move through the region, they find patches of upwelling/downwelling and consequently move up or down. To study this behaviour, we have computed the streamlines of the three-dimensional velocity field composed by the horizontal geostrophic velocity and *w*. The streamlines were determined by linearly interpolating the velocity field onto the location of the water parcels and integrating forward in time to find the next water parcel's position. In the case of a stationary field, the streamlines match the water parcels' trajectories. The trajectories for three water parcels initially launched within the core of the jet at 100 dbar are shown in Figure 7. Although the water parcels have crossed areas with *w* ranging from -20 m/day to 40 m/day, the net vertical displacements are less than 30 m in the period that the parcels spent in the sampled region. Water parcel (a) was initially released at the centre of the AJ. Hence it crossed the region in just 2.5 days, being advected from an upwelling maximum (which explains the initial fast raise) to the weak downwelling feature of the north part of the gyre, finally going back to the upwelling pattern that dominates the *w* field. The net upward displacement was 29 m in 2.5 days. On the other hand, water parcel (c) was released 10km north of (a), and hence was initially located in the northern part of the AJ. The weaker velocities forced the water parcel to take 5.5 days to cross the domain. It spent more time within the downwelling patch of the north than in the dominant upwelling feature, so its net upward displacement was just 10 m in 5.5 days

DISCUSSION AND CONCLUSION

A high-resolution survey of the north western Alborán sea was performed as part of the 1996 Omega project. The unprecedented resolution and synopticity of the survey provided a unique oppor-

tunity to diagnose vertical velocities using the quasi-geostrophic omega equation, in a dataset expressly designed for that purpose.

The density field shows a density front associated with the northern part of the WAG and the AJ, with gradients up to 2 kg m^{-3} in one Rossby radius. The ADCP absolute velocities show an AJ with maximum speeds above 110 cm/s, extending down to 200 dbar. A strong non-geostrophic circulation is associated with this frontal situation. We have diagnosed vertical velocities ranging from –20m/day to +40 m/day, the maximum values being placed within the AJ. As indicated in sections 4 and 5, the resulting *w* field is the consequence of an ocean in near geostrophic and hydrostatic balance. Therefore, the diagnosis of *w* in this complicated balance was carried out by the inversion of the quasi-geostrophic omega equation. Moreover, the isopycnal's slope by itself cannot suggests the *w* distribution. In the case presented here, the *w* field tends to displace upward light water and downward dense water, a way to increase the stratification.

Previous experiments carried out in the western Alborán sea have also inferred vertical motion from observations. Viúdez *et al*., (1996a,b) estimated quasigeostrophic vertical velocities up to 20 m/day, the maximum values corresponding to mesoscale meanders in the WAG. These estimates are lower than those diagnosed here, a consequence of the higher resolution of the data set used in the present study and therefore of the stronger density gradients found. In the western Alborán sea Tintoré *et al*. (1991) found vertical velocities up to 50 m/day, that were within the range of the estimates of the present study.

Analysis of the water parcel's trajectories indicates that the net vertical excursions depend on the initial position of the water parcel, ranging from 29 m in 2.5 days for water particles in the core of the jet to 9 m in 5.5 days for those in the boundaries of the jet. This is coherent with the quasi-geostrophic assumption that the vertical displacements are much smaller than the horizontal ones. These diagnostics should be used with care as they are just a snapshot of the real world, and the time-varying structures can significantly modify the upwelling and downwelling areas. Therefore, quantification of the transport of any quantity should be done with a precise knowledge of the four-dimensional (space and time) velocity field.

In summary, in a biological sense, the asymmetry imposed by the light field (in the euphotic layer) rectifies vertical displacements (both up and down) into a net upward transport of nutrients (McGillicuddy *et al*., 1998). Therefore, to understand the role of mesoscale activity in the ecosystem, we need to be able to know the vertical velocity field. Although the vertical velocities cannot be measured, they can be diagnosed trough an indirect method based on the quasi-geostrophic theory: the Omega equation. This equation can be solved from the three-dimensional density field. In the present study we have shown that this is indeed possible from routinely measured density data. It is the first time, as far as we know, that *w* has been diagnosed with a data set expressly designed to validate the indirect estimation methods for *w*. Complementary studies done by the authors have examined the sensitivity of the method to different parameters and dynamical situations found in the western Alborán Sea (Vélez-Belchí et *al*., 1999) and compared the *w* diagnosis with *in-situ* data from Lagrangian floats able to measure vertical velocities (Gascard *et al*., 1999).

REFERENCES

Allen, J.T., D.A. Smeed, N. Crips, S. Ruiz, S. Watts, P.J.Vélez-Belchí, P.Jornet, O.Rius and A.Castellón. – 1997. Upper Ocean underway operation on BIO Hespérides Cruise OMEGA-ALGERS (cruise 36) using SeaSoar and ADCP. *Southampton Oceanographic Centre, Internal Report.*

Barton, E.D., J. Arístegui, P. Tett, M. Cantón, J. García-Braun, S. Hernández-León, L. Nykjaer, C. Almeida, J. Almunia, S. Ballesteros, G. Basterretxea, J. Escánez, L. Garcia-Weill, A. Hernández-Guerra, F. López-Laatzen, R. Molina, M.F. Montero, E. Navarro-Pérez, J.M. Rodríguez, K. Van Lenning, H. Vélez and K. Wild. – 1998. The transition zone of the Canary Current upwelling region. *Progr. Oceanogr.,* 41: 455-504.

Blanco, J.M., F. Echevarría and C.M García. – 1994. Dealing with size spectra: some conceptual and mathematical problems. *Sci. Mar*., 58(1-2): 17-29.

Cano, N. and F. de Castillejo. – 1972. Contribución al conocimiento del mar de Alborán III. Variaciones del remoliono anticiclónico. *Bol. Inst. Esp. Oceanogr.,* 157: 3-7.

Dewey, R.K., J.N. Moum, C.A. Paulson, D.R. Caldwell and S.D. Pierce. – 1991. Structure and dynamics of a coastal filament. *J. Geophys. Res*., 96: 14885-14907.

Flament, P., L. Armi and L. Washburn. – 1985. The evolving structure of an upwelling filament. *J. Geophys. Res*., 90: 11765-11778.

Gascard, J.C. and C. Richez. – 1985. Water masses and circulation in the western Alborán Sea and in the Straits of Gibraltar. *Progr. Oceanogr*., 15: 157-216.

Gascard, J.C., J. Tintoré, P. Vélez-Belchí and R. Haney. – 1999. In situ observations of W from neutrally buoyant rotating floats during the Alborán OMEGA experiment and model intercomparisons. *31st International Liege Colloquium on Ocean Hydrodynamics, three-dimensional ocean circulation: Lagrangian measurements and diagnostic analyses.*

Gill, A.E. – 1982. *Atmosphere-Ocean dynamics*. Academic Press.

Holton, J.R. – 1992. *An introduction to dynamic Meteorology*. Academic Press.

Hoskins, B.J., I. Draghici and H.C. Davis. – 1978. A new look at the omega-equation. *Quart. J. Roy. Met. Soc*. 104: 31-38.

Hoskins, B.J., M.E. McIntyre and A.W. Robertson. – 1985. On the use and significance of isentropic potential vorticity maps. *Quart. J. Roy. Met. Soc*.,111, No. 470: 877-946.

Huyer, A. – 1976. A comparison of upwelling events in two loca-

tions: Oregon and Northwest Africa. *J. Mar. Res*., 34: 531-546.
Lanoix, F. – 1974. Projet Alborán, Etude hydrologique et dynamique de la Mer d´Albora. *Tech. Rep. 66, Nato*.
Leach, H. – 1987. The diagnosis of synoptic-scale vertical motion in the seasonal thermocline. *Deep-Sea Res.* 34: 2005-2017.
Lindstrom, S. and D.R. Watts. – 1994. Vertical motion in the Gulf Stream near 68ºW. *J. Phys. Oceanogr*., 24: 2321-2333.
McGillicuddy, D.J., A.R. Robinson, D.A. Siegel, H.W. Jannasch, R. Johnson, T. D. Dickey, J. McNeil, A.F. Michaels and A.H. Knap. – 1998. Influence of mesoscale eddies on new production in the Sargasso sea. *Nature*, 394: 263-265.
Mittelstaedt, E. – 1983. The upwelling Area off Northwest Africa – A description of phenomena related to coastal upwelling. *Progr. Oceanogr.,* 12: 307-331.
Onken, R. – 1992. Mesoscale upwelling and density finestructure in the seasonal thermocline—A dynamical model. *J. Phys. Oceanogr*., 22: 1257-1273.
Pedder, M.A. – 1989. Limited area kinematic analysis by a multivariable statistical interpolation method. *Mon. Wea. Rev*., 117: 1695-1708.
Pedder, M.A. – 1993. Interpolation and filtering of spatial observation using succesive corrections and gaussian filters. *Mon. Wea. Rev*., 121: 2889-2902.
Pinot, J.M., J. Tintoré, J.L. López-Jurado, M.L. Fernández de Puelles and J. Jansá. – 1995. Three-dimensional circulation of a mesoscale eddy/front system and its biological implications. *Oceanologica Acta*., 18: 389-400.
Pinot, J. M., J. Tintoré and D.P. Wang. – 1996. A study of the omega equation for diagnosing vertical motions at ocean fronts. *J. Mar. Res*., 54: 239-259.
Robinson, A. – 1983. *Eddies in the Ocean*. Springer-Verlag.
Ruíz, J., C.M. García, and J. Rodríguez. – 1996. Vertical patterns of phytoplankton size distribution in the Cantabric and Balearic Seas. *J. Mar. Sys*., 9: 269-282.
Strass, V.H. – 1992. Chlorophyll patchiness caused by mesoscale upwelling at fronts. *Deep-Sea Res*., 30, 1A: 75-96.
Strass, V.H. – 1994. Mesoscale instability and upwelling. Part 2: Testing the diagnostics of vertical motion with a three-dimensional ocean front model. *J. Phys. Oceanogr.,* 24: 1759-1767.
Tintoré, J., D. Gomis, S. Alonso and G. Parrilla. – 1991. Mesoscale dynamics and vertical motion in the Alborán Sea. *J. Phys. Oceanogr.,* 21: 811-823.
Vélez-Belchí, P., J. Allen, V.H. Strass and R.T. Pollard. – 1998. MVBS patchiness in the southern polar front. *Deep Sea Res I.* (submitted)
Vélez-Belchí, P., J. Tintoré, R.L. Haney and J.T. Allen. – 1999. Observations and diagnostic modelling of three-dimensional fields in an upper ocean front. *31st International Liege Colloquium on Ocean Hydrodynamics, three-dimensional ocean circulation: Lagrangian measurements and diagnostic analyses.*
Viúdez, A., J. Tintoré and R.L. Haney. – 1996a. Circulation in the Alborán Sea as determined by quasi-synoptic hydrographic observations. I. Three dimensional structure of the two anticyclonic gyres. *J. Phys. Oceanogr*., 26: 684-705.
Viúdez, A., J. Tintoré and R.L. Haney. – 1996b. Circulation in the Alborán Sea as determined by quasi-synoptic hydrographic observations. II. Mesoscale ageostrophic motion diagnosed through density dynamical assimilation. *J. Phys. Oceanogr*., 26: 706-724.
Williams, R.G. and M.J. Follows. – 1998. Eddies make ocean deserts bloom. *Nature*, 394: 228-229.
Wang, D.-P. – 1993. Model of frontogenesis: subduction and upwelling. *J. Mar. Res*. 51: 497-513.
Wang J. and M. Ikeda. – 1997. Diagnosing ocean unstable baroclinic waves and meanders using the quasigeostrophic equations and Q-vector method. *J. Phys. Oceanogr*., 27: 1158-1172.